SEMARAK ILMU PUBLISHING

Journal of Advanced Research in Applied Sciences and Engineering Technology

Journal homepage:
https://semarakilmu.com.my/journals/index.php/applied_sciences_eng_tech/index
ISSN: 2462-1943

Development and Fabrication of MOSFET-Based Radiation Dosimeter (RadFET) for Enhanced Performance in Space Missions

Dalia Elfiky[1,*], Ahmed S. Abd-Rabou[2], Haitham Akah[1], Ayman Mahmoud[3], Kirollos Ernest[2], AbdelRahman Mohamed[2], Alaa M. Ali[2], AbdelRahman Elshorbagy[3], Shaimaa Mohamed[2], Amr M. Bayoumi[2]

[1] National Authority for Remote Sensing and Space Science, Cairo, Egypt
[2] Nanotechnology and Nanoelectronics Engineering Program, University of Science and Technology, Zewail City of Science, Technology and Innovation, October Gardens, Giza 12578, Egypt
[3] Egyptian Space Agency, Egypt

ARTICLE INFO

Article history:
Received 13 July 2023
Received in revised form 2 October 2023
Accepted 19 December 2023
Available online 7 February 2024

Keywords:
Radiation dosimeter; Space missions; Device simulation

ABSTRACT

This work presents the development and fabrication process of a radiation dosimeter based on Metal-Oxide-Semiconductor Field-Effect Transistor (MOSFET) technology, known as RadFET. The aim of this study is to determine the specifications of the RadFET sensor for use in space missions by the Egyptian Space Agency in SPNeX mission. We have successfully determined the sensor specifications, specified the required electronic components for readout circuits, and confirmed the correct operation of the RadFET device through device simulations and radiation-induced damage models. The fabrication process was conducted at Zewail City of Science, Technology and Innovation cleanroom facility, utilizing Sentaurus TCAD for device and process simulations. We have conducted fabrication experiments for phosphorus spin-on dopant application, dry oxide growth, and wet oxidation using water vapor bubblers. The dosimeter readout PCB fabrication and assembly phases have been successfully completed. The developed RadFET dosimeter holds great promise for radiation monitoring in space missions, ensuring enhanced safety and reliability of electronic systems.

1. Introduction

Radiation dosimeters play a critical role in space missions, where exposure to high levels of radiation poses significant risks to both human astronauts and electronic systems. Accurate and reliable radiation measurement is essential for assessing the potential impact of radiation on mission success and crew safety.

Radiation dosimetry is of paramount importance in space missions, due to the elevated levels of ionizing radiation in space, posing significant health risks to astronauts and electronic systems. To address this challenge, Metal-Oxide-Semiconductor Field-Effect Transistors (MOSFETs), particularly RadFETs (Radiation-Sensitive Field-Effect Transistors), have emerged as promising candidates for

* *Corresponding author.*
E-mail address: delfiky@narss.sci.eg

https://doi.org/10.37934/araset.39.1.135148

radiation dosimetry in space missions. RadFETs offer compactness, high sensitivity, and compatibility with integrated circuit fabrication, making them well-suited for space applications, as mention in [1]. The use of semiconductor devices for radiation dosimetry in space missions has a rich history, with early experiments involving silicon diodes and transistors. Over time, specialized radiation-sensitive devices like RadFETs have been developed and extensively studied. Research in this field has focused on calibrating RadFETs to various radiation levels, characterizing their behaviour under different radiation types, and developing readout circuits and data analysis techniques to extract radiation dose information, as reference in [2]. The advantages of semiconductor-based dosimetry include real-time monitoring, compact form factors, and low power consumption, which are vital for long-duration space missions, as indication in [3]. Despite their promise, these dosimeters face challenges like radiation-induced damage, necessitating precise calibration. Future research aims to address these challenges, optimize dosimeter designs, and develop space-ready dosimetry systems, as remark in [4]. The integration of semiconductor-based dosimeters into spacecraft and satellite components is a practical approach, providing continuous radiation data essential for astronaut safety and mission success, as state in [5].

Various research studies have focused on optimizing the performance of RadFET devices, developing fabrication techniques, and characterizing their radiation response. These advancements have paved the way for the utilization of RadFET dosimeters in space missions and other radiation-sensitive applications, as declare in [2].

One key aspect of RadFET development is the determination of sensor specifications tailored to the requirements of space missions. Previous studies have explored the influence of device parameters, such as channel length, gate oxide thickness, and substrate doping concentration, on the dosimeter's sensitivity and radiation response. These investigations have contributed to the optimization of RadFET designs for enhanced performance in harsh radiation environments, as mention in [3-5].

Furthermore, the design and fabrication of readout circuits are critical for accurate radiation dose measurement. Research efforts have focused on developing efficient readout circuits capable of capturing and processing the signal generated by the RadFET sensor. These circuits often incorporate analogue front-end components, signal amplification stages, and digital interfaces for data acquisition and analysis. The integration of these circuits with the RadFET sensor allows for real-time radiation monitoring and data transmission, as citied in [6-9].

Process simulation and device modelling have also played a crucial role in the development of RadFET dosimeters. By utilizing tools such as Technology Computer Aided Design (TCAD), researchers have been able to simulate the device behaviour, analyse radiation-induced effects, and optimize fabrication processes. TCAD simulations provide insights into the device's electrical characteristics, such as threshold voltage shifts, leakage currents, and charge trapping phenomena, enabling the design of robust and accurate dosimeters, as discussed in [10-12].

While significant advancements have been made in RadFET dosimetry, challenges still exist, including contact resistance, oxide leakage, and accurate wafer doping. Addressing these challenges is crucial to ensure the reliability and accuracy of the dosimeter's performance. Additionally, the successful fabrication and assembly of the dosimeter, including the readout PCB, is essential for its integration into space missions.

The objective of this study is to develop and fabricate a radiation dosimeter based on MOSFET technology, known as RadFET, for use in space missions by the Egyptian Space Agency.

Also, we aim to contribute to the existing body of knowledge by determining the specifications of the RadFET sensor, optimizing the fabrication process, and validating the dosimeter's performance through simulations and experiments. The successful development and fabrication of the RadFET

dosimeter will pave the way for its utilization in space missions, ensuring effective radiation monitoring and contributing to the safety and reliability of future space exploration endeavours.

2. Methodology

This section outlines the methodology employed in the development and fabrication of the RadFET radiation dosimeter. The methodology encompasses various steps, including sensor specification determination, fabrication process optimization, and performance validation through simulations and experiments.

2.1 Sensor Specifications Determination

The first phase of the methodology involves determining the specifications of the RadFET sensor specifically tailored for space missions. This process incorporates a comprehensive analysis of the radiation environment in space, considering factors such as radiation type, energy levels, and expected dose rates. Through careful evaluation and iterative refinement, the sensor specifications, including channel length, gate oxide thickness, and substrate doping concentration, are determined to ensure optimal sensitivity, radiation response, and overall performance in space conditions.

2.2 Device Radiation Model

In the second phase, Sentaurus software by Synopsys simulated the behaviour of the PMOS device under combined surface and bulk radiation damage. This aimed to understand radiation's impact on electrical traits like threshold voltage shifts, leakage currents, and charge trapping.

Sentaurus accurately modelled the PMOS device's response to radiation damage, considering both surface and bulk effects. The simulation process included defining the device model, integrating radiation damage models, analysing radiation doses and energies, running simulations, and evaluating results.

Radiation alters device behaviour through ionization, creating electron-hole pairs, and atomic displacement, forming vacancy-interstitial atom pairs. It also heightens trap density at material interfaces, presenting allowed states in the forbidden bandgap. These traps can be acceptors or donors, some of which are above midgap. Traps are characterized by concentration, capture cross sections, energy distribution, and allocation—uniform, Gaussian, or specific levels.

2.2.1 Radiation in MOS devices

Generally, MOS devices are more sensitive to ionizing effect. Generated electron-hole pairs recombine faster in silicon substrate and metal gate, while effect persists in silicon dioxide layer. Part of generated carriers transport under influence of electric field in dioxide layer to reach Si/SiO_2 interface, most of them are trapped holes creating a fixed positive charge at oxide interface. Radiation induced traps in MOS devices are allocated near Si/SiO_2 interface. In order to classify radiation damages in MOS devices, two main damage categories will be discussed in this work: surface damage meant by damage in Si/SiO_2 interface caused by ionizing effects and atomic displacements and bulk damage caused by atomic displacements.

2.2.2 Technology radiation model

Radiation induced damage characteristics are function in technology parameters like wafer doping, wafer orientation and wafer growth technique. Also, depending on type of radiation that hits the device. Many models are developed to describe damage parameters in silicon MOS devices describing operation of RADFETs under certain fluences or dose. Bulk damages are usually described as function of fluence (particles/area) while surface damages are referred to dose (rad). Fluence and dose are related by equation given by CERN for 50 Mrad = 10^{15} n_{eq}/cm^2.

2.2.3 Surface radiation damage

Surface radiation damage models introduced in literature are oxide positive fixed charge Qox (cm^{-2}), acceptor interface trap states N_{ITacc} (cm^{-2}), donor interface trap states N_{ITdon} (cm^{-2}). Pre-irradiations values represents these quantities when there is no radiation. Table shows the fitting equations and pre-irradiation values provide by Perugia 2019 surface model [11]

Table 1
The fitting equations and pre-irradiation values provide by Perugia 2019 surface model [11]

Fitting Equations	Pre-irradiation Values
$\Delta Q_{OX} = 3.74 \times 10^{+11} + 6.20 \times 10^{+10} \cdot \ln \emptyset$	$Q_{OX}(0) = 6.5 \times 10^{+10}$
$\Delta N_{IT_{OX}} = 6.35 \times 10^{+11} + 1.50 \times 10^{+11} \cdot \ln \emptyset$	$N_{IT_{acc}}(0) = 2.0 \times 10^{+10}$
$\Delta N_{IT_{don}} = 1.07 \times 10^{+12} + 2.90 \times 10^{+11} \cdot \ln \emptyset$	$N_{IT_{don}}(0) = 2.0 \times 10^{+9}$

Where,

$$Q_{OX}(\emptyset) = Q_{OX}(0) + \Delta Q_{OX}(\emptyset)$$
$$N_{IT_{acc}} = N_{IT_{acc}}(0) + N_{IT_{acc}}(\emptyset)$$
$$N_{IT_{don}} = N_{IT_{don}}(0) + N_{IT_{don}}(\emptyset)$$

Φ is dose given by (rad). The complete definition for interface traps requiring supplying the electron and hole capture cross sections, energy distribution and trap densities. Trap densities at surface are uniformly distributed over determined range inside the bandgap at determined distance from conduction band or valence band. The surface damage model for radiation induced traps is given in the Table .

Table 2
The surface damage model for radiation induced traps

	Acceptor-like	Donor-like
Energy (eV)	EC − 0.56 ≤ ET ≤ EC	EV ≤ ET ≤ EV + 0.60
Width (eV)	0.56	0.60
D_{IT} ($eV^{-1}cm^{-2}$)	$D_{IT_{acc}}(\emptyset)$	$D_{IT_{don}}(\emptyset)$
N_{IT} (Ø) (cm^{-2})	$N_{IT_{acc}}(0) + D_{IT_{acc}}(\emptyset)$	$N_{IT_{don}}(0) + D_{IT_{don}}(\emptyset)$
$\sigma_{electrons}$ (cm^2)	1.00x10^{-16}	1.00x10^{-15}
σ_{holes} (cm^2)	1.00x10^{-15}	1.00x10^{-16}
Fixed oxide charge		
Q_{OX} (Ø) (cm^{-2})	Q_{OX} (0) +Q_{OX} (Ø)	

2.2.4 Bulk radiation model

Bulk radiation damage is proposed in literature with three quantities: two discrete trap level of acceptor type and one discrete trap level of donor type. The concentration of generated traps is directly proportional to radiation fluence by a proportionality constant called introduction rate η (cm^{-1}).

Table shows typical parameters for bulk radiation induced traps. It's important to mention that bulk radiations are discrete level traps.

Table 3
The typical parameters for bulk radiation induced traps

Type	Energy Level [eV]	$\sigma_e[cm^{-2}]$	$\sigma_h[cm^{-2}]$	$\eta[cm^{-1}]$
Donor	E_V + 0.48	2x10^{-14}	1x10^{-14}	4
Acceptor	E_C + 0.48	5x10^{-15}	1x10^{-14}	0.75
Acceptor	E_V + 0.90	1x10^{-16}	1x10^{-16}	36

2.2.5 Radiation effects on MOS devices

Fixed charges and generated traps have several impacts on the electrical performance of MOS devices, most important parameter is the threshold voltage V_T shift leakage current and transconductance g_m.

Threshold voltage shifting ΔV_T under radiation can be divided into two components, shifting due to charges trapped in oxide ΔV_{ox}, the charges trapped in oxide cause a shift in flat band voltage. Second contributor is trapped charges at Si/SiO2 interface ΔV_{IT} due to traps states created. Trapped charges are directly proportional to oxide thickness. Increasing oxide thickness increase the sensitivity of MOS based RADFET.

2.2.6 Radiation model in Sentaurus TCAD

The following Table 4 define radiation parameters for Sentaurus workbench (swb). Three cases for fluences are studied in this work 10^{11}, 10^{13} and 10^{15}.

Table 4
Radiation parameters as defined in Sentaurus workbench [11]

	Fluence	Qox0	DQox	Nd0	DNd	Nacc	DNacc
[n1]: --	[n2]: 0	[n6]: 8.00E+10	[n10]: 0	[n14]: 9e+9	[n18]: 0	[n22]: 7e+9	[n26]: 0
	[n3]: 1e+11	[n7]: 8.00E+10	[n11]: 1.64E+12	[n15]: 9e+9	[n19]: 2.31e+12	[n23]: 7e+9	[n27]: 4.78e+12
	[n4]: 1e+13	[n8]: 8.00E+10	[n12]: 2.21E+12	[n16]: 9e+9	[n20]: 3.23e+12	[n24]: 7e+9	[n28]: 6.51e+12
	[n5]: 1e+15	[n9]: 8.00E+10	[n13]: 2.78E+12	[n17]: 9e+9	[n21]: 4.14e+12	[n25]: 7e+9	[n29]: 8.25e+12

The corresponding pre-irradiances and post irradiances values are shown in Table . The corresponding bulk and interface trap densities are shown in Table 5. The defined parameters are then used globally within all Sentaurus simulations.

Table 5
The corresponding bulk and interface trap densities

Qox	Dit_acc	Dit_don	ConcAcc1	ConcAcc2	ConcDon1
8.00e+10	7.00e+09	9.00e+09	0.00e+00	0.00e+00	0.00e+00
1.72e+12	4.79e+12	2.32e+12	1.60e+11	9.00e+10	9.00e+10
2.29e+12	6.52e+12	3.24e+12	1.60e+13	9.00e+12	9.00e+12
2.86e+12	8.26e+12	4.15e+12	1.60e+15	9.00e+14	9.00e+14

2.3 Fabrication Process Optimization

The second phase focuses on optimizing the fabrication process for the RadFET dosimeter. This step involves utilizing advanced process simulation tools, such as Sentaurus Sprocess, to model and refine the fabrication steps. By simulating various fabrication parameters, such as dopant diffusion techniques, oxide growth methods, and deposition processes, the optimal conditions for producing RadFET dosimeters with consistent performance and high yield are identified. The fabrication process is iteratively refined based on simulation results and experimental feedback.

2.3.1 Transistor specification

The target parameters of the transistor chosen for this study are summarized in **Error! Reference source not found.**, which are in-line with the values used in the literature:

Table 6
Target RadFET Transistor Specification

Parameter	Value
Transistor Type	PMOS
Length (L)	100 um
Width (W)	750 um
Channel Doping	1E15 cm-3
Gate Oxide Thickness	400 nm
Threshold Voltage	-3.5 V
Aluminium Gate Thickness	500 nm

2.3.2 Process flow

Fig. 1 shows the process flow. It depends heavily on spin-on-glass (SOG) dopant diffusion, as presented in [13-15]. The process starts with n-type 100 epitaxial wafers with 1E15cm^{-3} doping. The gate oxide thickness is 400 nm, grown by a dry-wet-dry oxidation cycle, as shown in **Error! Reference source not found.**. This oxide layer is also used as both gate oxide, as well as the first part of the field oxide. The first mask is used to define the Source/Drain and gate oxide regions (Fig. 1a).

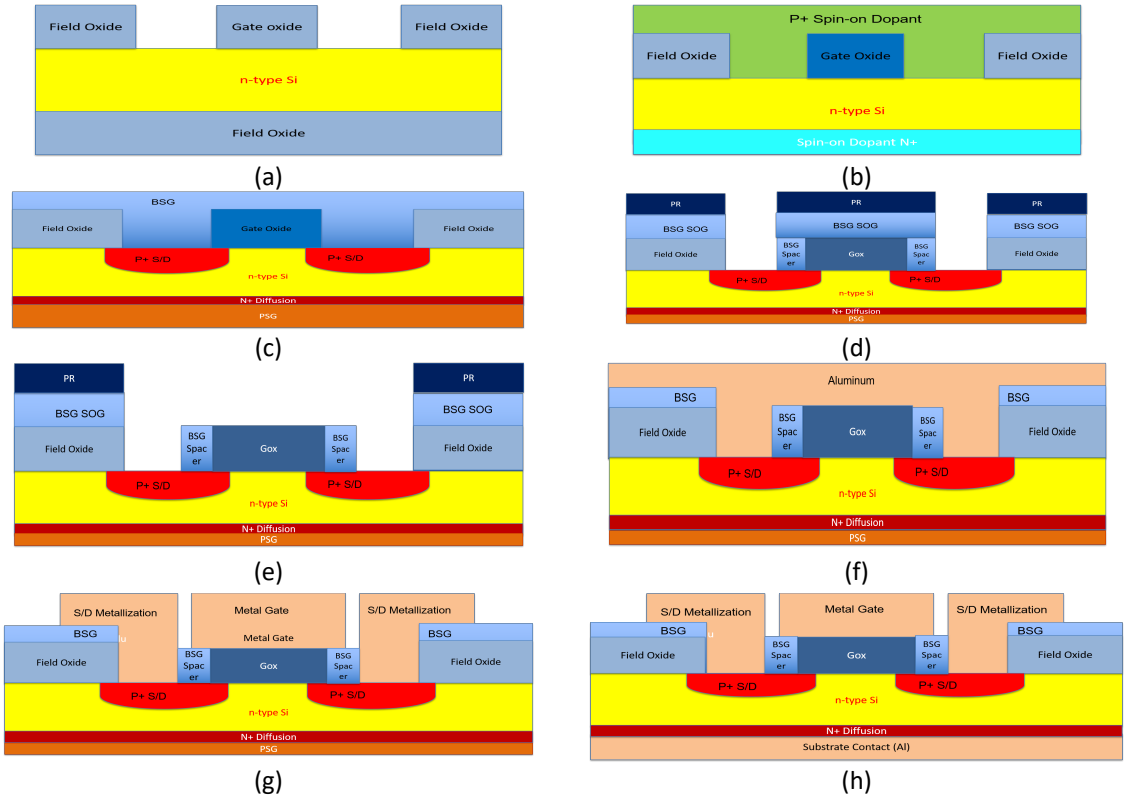

Fig. 1. Fabrication Process Steps

Table 7
Gate Oxidation Cycle

Gas	Temperature	Duration
O_2	900C	20 min.
H_2O	1000C	67 min.
O_2	900C	20 min.

This is followed by application of spin-on glass (SOG) dopant of boron for source drain, and SOG for phosphorus for the backside contact after backside oxide etch (Fig. 1b). A drive-in cycle is conducted to drive the source/drain and backside contacts (Figure 1c) as shown in **Error! Reference source not found.**. A second mask is used to define the active regions, where the SOG oxide, with thickness of 1000 nm, is used as the second layer of the field oxide (Fig. 1-d), in order to avoid the parasitic effect under the field oxide. This is done by etching the SOG oxide from all regions, except the field oxide (Fig. 1e). This is followed by a third mask to define the contacts to source/drain, followed by oxide etch till the silicon is reached. A Forming Gas Anneal (FGA) is conducted for 30 min at 450C in 5% H_2/N_2 , as mention in [16]. After that, Aluminium of 500 nm is deposited using evaporation (Fig. 1-f), followed by the fourth mask to define the metallization, including the metal gate, the source/drain contacts and the associated probing pads (Fig. 1-g). The backside oxide formed during SOG spinning and drive-in is then wet-etched, followed by backside metallization (Fig. 1-h). A final forming gas anneal is conducted at 300C, in order to minimize possible diffusion of Al into Si source/drain, as state in [16]. I-line lithography at 365 nm was used for 3x reduction projection lithography. UV ozone cleaning was conducted following hard baked photoresist strip.

Table 8
Diffusion Cycle

Gas	Temperature	Duration
N_2	950C	30 min.
O_2	1000C	30 min.

2.4 Readout Circuit Specifications

Readout circuits are vital for precise radiation dosimetry, converting signals from sensors like MOSFETs into analysable data. Their specifications influence dosimeter sensitivity, resolution, and range, crucial for detecting and quantifying radiation, as in reference [17]. We focus on optimizing RadFET dosimeter readout circuits, particularly for space missions. RadFETs are valued for sensitivity and compactness, driving the need for accurate readout. By honing circuitry, we enhance dosimeter performance, enabling real-time space radiation monitoring for safety and mission success.

As shown in Fig Key parameters include sensitivity, ADC resolution, and seamless mode switching. Sensitivity of 58.3 µV ensures precise dose measurement. A 20-bit ADC with 3.14 µV per bit resolution, and a 3.3V max range, guarantee fine voltage detection. Circuit design permits seamless shifts between sensing and reading modes. This critical interplay ensures accurate radiation readings, safeguarding astronauts and electronics during missions, as state in [18].

The readout circuit primarily functions as a precision current source, fuelling RadFET biasing for threshold voltage deduction. Two crucial specifications are detailed below:

i. Sensitivity (Resolution): The targeted sensitivity is 58.3 µV, enabling precise dose measurement and capturing subtle voltage changes.
ii. ADC Resolution and Max Range: A 20-bit ADC offers 3.14 µV per bit resolution, with a 3.3V range for voltage detection and digitization.
iii. Switching Modes: The readout circuit adeptly toggles between sensing and reading modes, vital for real-time radiation monitoring and accurate data transmission.

These specifications are paramount for RadFET dosimeter functionality, guaranteeing precise data acquisition and effective radiation dose assessment in space missions.

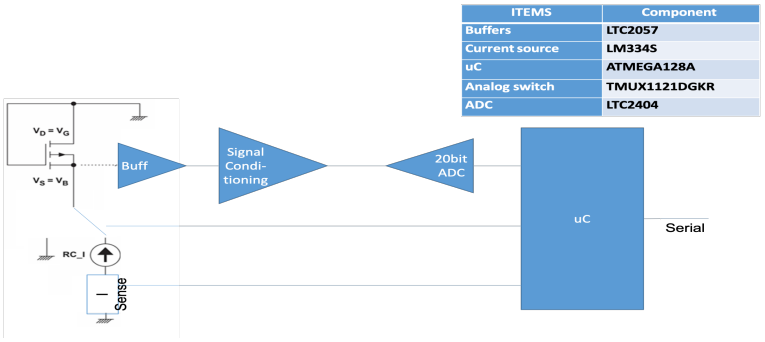

Fig. 2. adFET Readout block diagram

2.5 RadFET Interface Board

Satellite missions require robust dosimeters for continuous radiation monitoring. RadFET's compactness and sensitivity make it ideal. The Interface Board links RadFET to the CCU, ensuring seamless data transfer and mode switching, as state in [19-21].

This section details RadFET Interface Board's optimization for space dosimetry. It's designed for space's demands, from architecture to software layers. The CCU's embedded software handles events, protocols, and data, ensuring consistent dosimeter performance.

Interface Board connects RADFET to OBC via CCU. CCU, with an MSP430 microcontroller, runs configurable code across platforms.

CCU's core functions are depicted in Fig. **2** CCU Connections, integral for satellite's reliability.

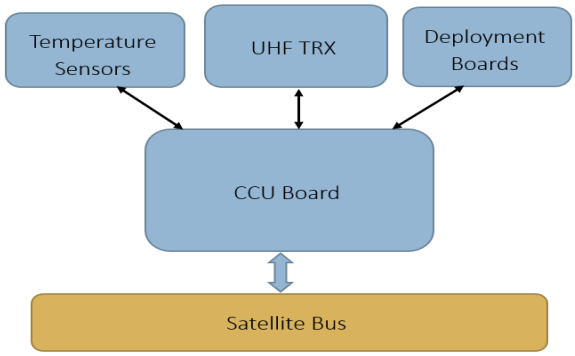

Fig. 2. CCU Connections

3. Results

3.1 Sensor Specifications

The RadFET dosimeter developed for space missions exhibits specific specifications that are crucial for accurate radiation measurement and reliable performance. **Error! Reference source not found.** presents the specifications that have been determined and optimized:

Table 9
The sensor specifications

Parameter	Value
Max Radiation dV	5.3V @ 100kRad
Pre-radiation voltage at biasing current	5.3V @ 100kRad
Pre-radiation voltage at biasing current	1.5V
Max Radiation voltage (100kRad accumulation)	7V
EgSA required Sensitivity (resolution)	58.3uV
1.1Rad voltage	58.3uV
ADC max range	3.3V
ADC resolution: 20bit	3.14 uV
Rad voltage after 1:2.25 scale down	25.9uV > ADC resolution
	Switching between sensing mode and reading mode

3.2 PMOS Simulation

3.2.1 Process TCAD simulations

Error! Reference source not found. shows the main structure features using TCAD simulations. This figure shows a cross section of the simulated structure, showing the silicon n-type substrate (in Red), the source/drain p+ diffused junctions using boron (in blue, with dark blue indicating a heavier doping), the 600nm gate oxide (in brown), and the metallization over the gate and source/drain regions (in grey). This structure is then used by the Device TCAD simulator to examine the electrical properties.

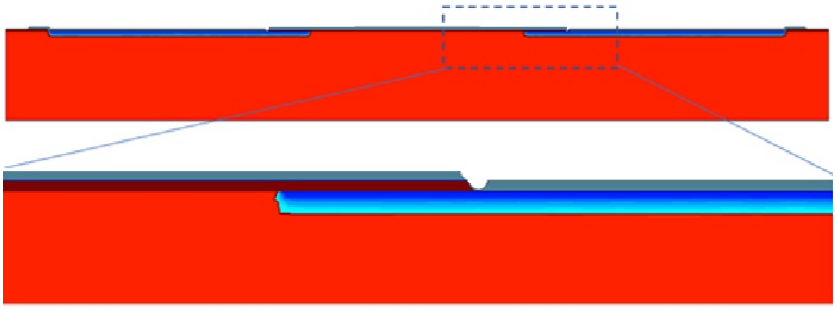

Fig. 4. The main structure features using TCAD simulations

3.2.2 Device TCAD simulations

Starting by performing I-V characteristics for the proposed RADFET-PMOS proposed in the previous section. In order to extract the initial threshold voltage and the shift in the threshold voltage induced by the radiation, the Id-Vg relation is extracted by performing DC sweeps in Sentaurus. Fig. **3** shows the Id- Vg relation for the PMOS with SiO_2 gate oxide. Another Fig. **4** to be investigated is the Id-Vd relation, the proposed RADFET has almost constant drain current under no radiation, the radiation causes an increase in the drain current with the drain voltage as shown in Fig. **4**

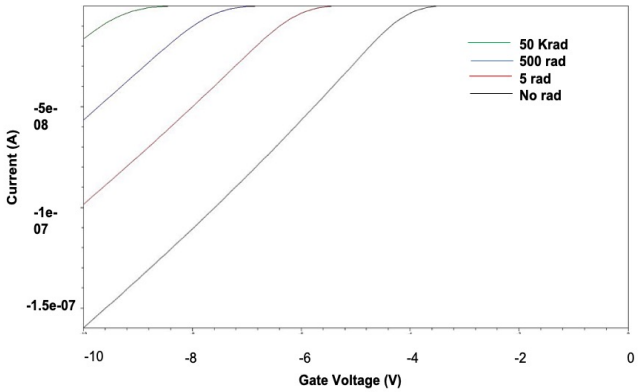

Fig. 3. Id-Vg relation for SiO2 gate stack

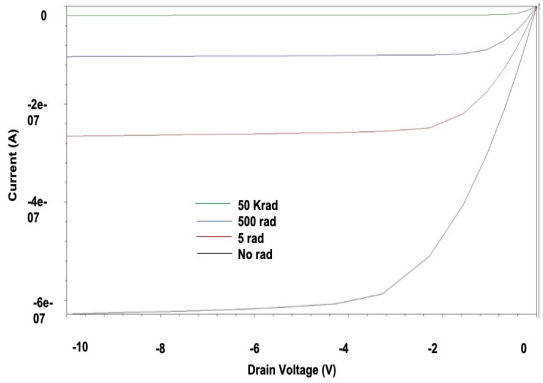

Fig. 4. Id-Vd for SiO2 gate stack

The C-V relations under radiation effects are shown in Fig. 5. The corresponding shifting in threshold voltage under influence of radiation can be extracted by calculating the threshold voltage for each curve as shown in Fig. 6.

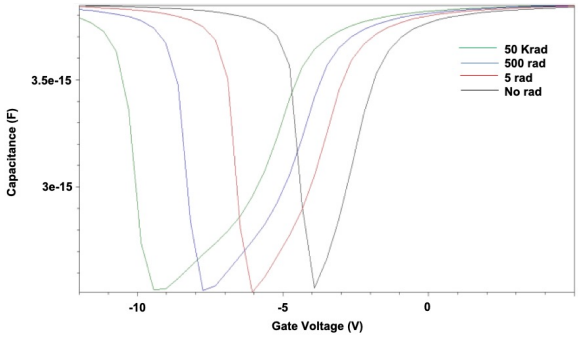

Fig. 5. Radiation effects on C-V relations

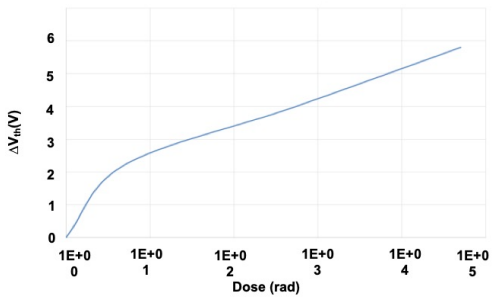

Fig. 6. The change of threshold voltage under influence of radiation dose

3.3 RADFET Transistor

The VLSI layout for the RADFET is shown in Fig. 7a, while Fig. 7b shows the mask layout used for 3x projection lithography. One mask plate was used for the 4 mask levels, by rotating 90 degrees. Three RadFETs were fabricated on each structure.

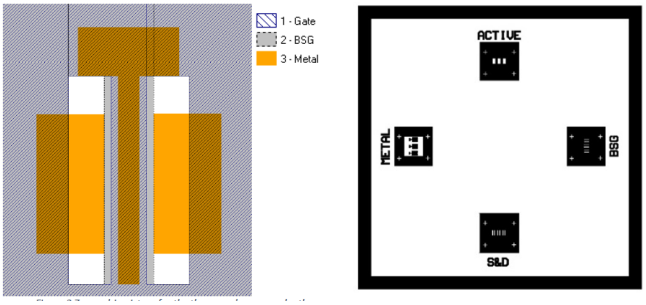

(a) (b)

Fig. 7. (a) Transistor layout and (b) Mask used for 3X projection lithography

Fig. 8a shows the transistor with photoresist prior to metal etching, while Fig. 8b shows the RADFET after full fabrication till metal contacts.

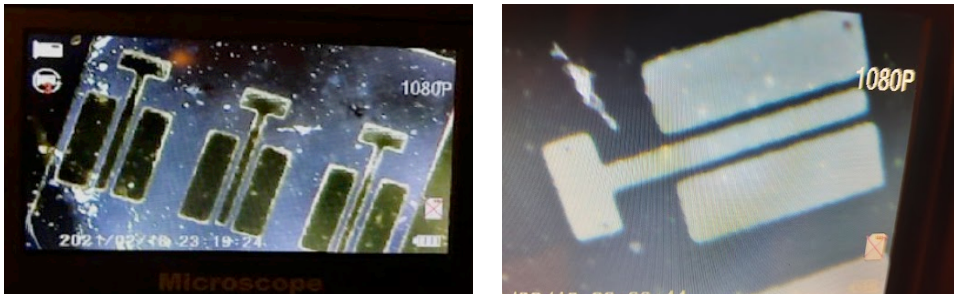

(a) (b)

Fig. 8. The transistor with photoresist (a) prior to and (b) after metal etching

3.4 Readout Board

Fig. 9 shows the assembled readout board, which will be used in conjunction with the off-the-shelf transistors and the in-house fabricated RadFET.

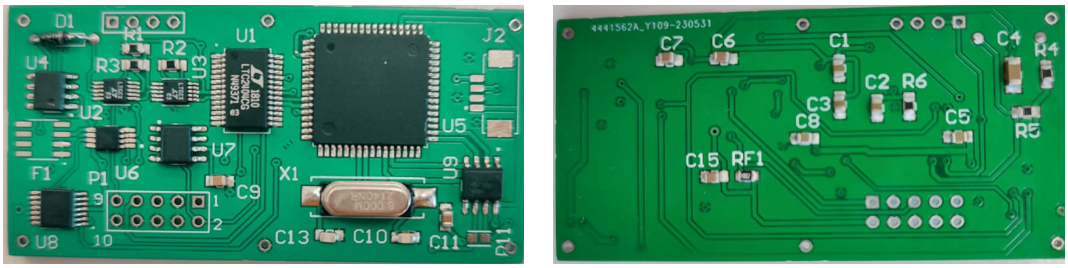

(a) (b)

Fig. 9. The assembled readout board: (a) Front side and (b) Back side

3.5 RadFET Interface Board

3.5.1 Physical architecture

The CCU Board consists of many interfaces as shown in Fig. 10 and Fig. 11, the main control unit is a MSP430 Microcontroller which will interface with RADFET device and other devices such as temperature sensors through I2C interface.

The CCU subsystem is also interface with other subsystems on the satellite stack through a two RS435 channels, one is the main and the other is redundant for high availability

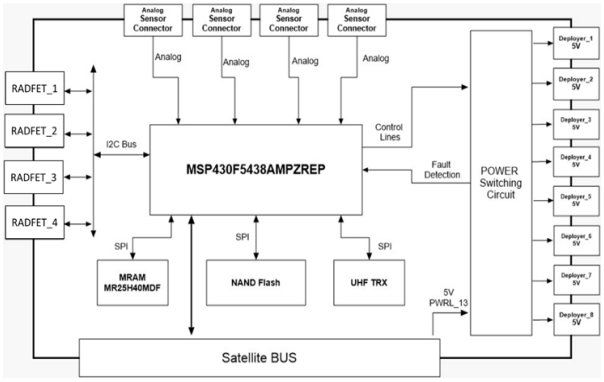

Fig. 10. CCU Interfaces

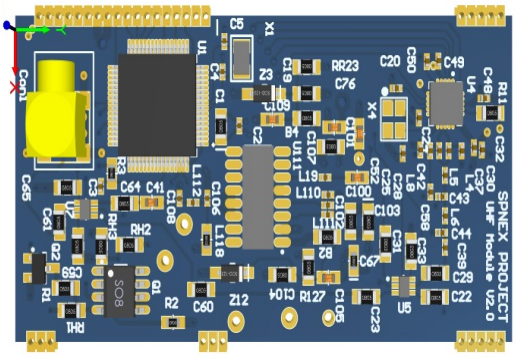

Fig. 11. PCB board

The Module Controller has:

i. Interface with SPI channel.
ii. It also has some control GPIO pins.
iii. CCU software components:

This includes an event handler task which is responsible for handling various events such as new SSP frames received, new SSP frames to be transmitted, timeout events, sync counter, sync pulse to OBC, sync pulse from OBC, deployment handler, and TLM handler. It also includes a protocol handling task which only handles the SSP protocol, consisting of SSP packing, SSP unpacking, and SSP handler.

4. Conclusions

In this study, we have developed and fabricated a radiation dosimeter based on Metal-Oxide-Semiconductor Field-Effect Transistor (MOSFET) technology, known as RadFET, for utilization in space missions by the Egyptian Space Agency. The RadFET dosimeter offers advantages such as real-time monitoring, compactness, and low power consumption, making it ideal for space applications. The methodology involved determining the RadFET sensor specifications optimized for space missions and validating its performance through simulations and experiments. TCAD simulations allowed us to analyse the effects of radiation on the PMOS device, including threshold voltage shifts and leakage currents. The fabrication process was optimized using advanced process simulation tools to achieve consistent performance and high yield. The readout circuit specifications, including sensitivity, ADC resolution, and range, were carefully designed to ensure accurate data acquisition and radiation dose measurement. The successful development and fabrication of the RadFET dosimeter hold promise for its integration into space missions, enabling effective radiation monitoring and ensuring the safety and reliability of astronauts and electronic systems. Despite some challenges like contact resistance

and oxide leakage, further research and improvements will pave the way for its successful implementation in future space exploration endeavours. The RadFET dosimeter represents a significant advancement in radiation dosimetry, offering real-time monitoring and compact design, making it an essential tool for assessing the radiation environment in space and safeguarding the well-being of space missions and crew members.

Looking ahead, the potential applications of the RadFET dosimeter extend beyond space missions. Future research avenues could explore its implementation in terrestrial environments with high radiation exposure, contributing to advancements in medical radiation monitoring and industrial safety. The adaptability of the RadFET technology opens up exciting possibilities for its integration into various fields, further solidifying its role as a cutting-edge solution in radiation dosimetry.

Acknowledgement
This work is supported by the Information Technology Industry Development Agency (ITIDA) – Information Technology Academia Collaboration (ITAC) program under grant number CFP204.

References

[1] x

References

[1] Holmes-Siedle, A., & Adams, L. (1986). "RADFET: A review of the use of metal-oxide-silicon devices as integrating dosimeters." International Journal of Radiation and Applications in Instrumentation. Part C Radiation Physics and Chemistry, 28(2), 235–244. doi: 10.1016/1359-0197(86)90134-7.
[2] Lee, N. H., Cho, J. W., Kim, S. H., & Youk, G. U. (2000). "Development of Electronic Radiation Dosimeter Using Commercial Power pMOSFET." Journal of Nuclear Science and Technology, 37(Suppl. 1), 803–807. doi: 10.1080/00223131.2000.10875001.
[3] Karmakar, Arijit, Jialei Wang, Jeffrey Prinzie, Valentijn De Smedt, and Paul Leroux. 2021. "A Review of Semiconductor Based Ionising Radiation Sensors Used in Harsh Radiation Environments and Their Applications" Radiation 1, no. 3: 194-217. https://doi.org/10.3390/radiation1030018.
[4] Kaya, S., Jaksic, A., Duane, R., Vasovic, N., & Yilmaz, E. (2018). "FET-based radiation sensors with Er2O3 gate dielectric." Nuclear Instruments and Methods in Physics Research Section B: Beam Interactions with Materials and Atoms, 430, 36–41. doi: 10.1016/j.nimb.2018.06.007.
[5] Pejović, S. M., Pejović, M. M., & Živanović, M. (2019). "Small dose effect in RADFET with thick gate oxide." Applied Radiation and Isotopes, 152, 72–77. doi: 10.1016/j.apradiso.2019.06.034.
[6] Morozzi, A., Moscatelli, F., Croci, T., Passeri, D. (2021). "TCAD Modeling of Surface Radiation Damage Effects: A State-Of-The-Art Review." Frontiers in Physics, 9. doi: 10.3389/fphy.2021.617322.
[7] Andjelkovic, Marko, Aleksandar Simevski, Junchao Chen, Oliver Schrape, Zoran Stamenkovic, Milos Krstic, Stefan Ilic, Goran Ristic, Aleksandar Jaksic, Nikola Vasovic, Russell Duane, Alberto J. Palma, Antonio M. Lallena, and Miguel A. Carvajal. "A Design Concept for Radiation Hardened RADFET Readout System for Space Applications." Microprocessors and Microsystems 90 (2022): 104486. ISSN 0141-9331. https://doi.org/10.1016/j.micpro.2022.104486.
[8] Ferraro, R., et al. (2017). "Design of a Radiation Tolerant System for Total Ionizing Dose Monitoring Using Floating Gate and RADFET Dosimeters." Journal of Instrumentation.
[9] Simevski, A., Kraemer, R., Krstic, M. (2011). "Low-Complexity Integrated Circuit Aging Monitor." Proceedings of IEE Symposium on Design and Diagnostics of Electronic Circuits and Systems (DDECS).
[10] Unno, Y., Ikegami, Y., Kohriki, T., Terada, S., Hara, K., Yamamura, K., et al. (2011). "Optimization of surface structures in n-in-p silicon sensors using TCAD simulation." Nucl Instrum Methods Phys Res A, 636, S118–S124. doi: 10.1016/j.nima.2010.04.095.
[11] Jain, G. (2019). "Radiation damage modeling: TCAD simulation." RD50 Collaboration, 12 p, PoS VERTEX2018 (2019) 017. doi: 10.22323/1.348.0017.
[12] SentaurusTM Device User Guide, Version O-2018.06, June 2018.
[13] Liu, Y., et al. (2017). "An experimental study of solid source diffusion by spin on dopants and its application for minimal silicon-on-insulator CMOS fabrication." Japanese Journal of Applied Physics, 56(6). doi: 10.7567/JJAP.56.06GG01S.

[14] Liu, Y., Khumpuang, S., Nagao, M., Matsukawa, T., & Hara, S. (2016). "Fabrication of PVD-TiN metal-gate SOI-CMOS integrated circuits using minimal-fab and mega-fab hybrid process." 2016 IEEE 16th International Conference on Nanotechnology (IEEE-NANO). doi: 10.1109/NANO.2016.7751371.
[15] Meier, A., Wolf, S., Mack, S., Lohmüller, S., & Glunz, S. W. (2018). "Role of Oxygen for Boron Diffusion From Borosilicate Glass Layers Deposited by Atmospheric Pressure Chemical Vapor Deposition." IEEE Journal of Photovoltaics, 8(4), 982-989. doi: 10.1109/JPHOTOV.2018.2835445.
[16] Campbell, S. A. (2008). "Fabrication Engineering at the Micro and Nanoscale." Oxford University Press, 3rd Ed..
[17] Andjelkovic, M., et al. (2020). "Design of Radiation Hardened RADFET Readout System for Space Applications." 2020 23rd Euromicro Conference on Digital System Design (DSD). doi: 10.1109/DSD51259.2020.00082.
[18] Ullah, S., et al. (2021). "A fully integrated radFET dosimeter for radiation measurement in space." Proceedings of the 2021 International Conference on Artificial Intelligence in Electronics Engineering (ICAIEE). doi: 10.1145/3461890.3461899.
[19] Melinger, J., & Barrientos, G. (2017). "The RADES Dose Sensor as a Tool for Space Radiation Studies." Aerospace Conference, 2017 IEEE, 1-12. doi: 10.1109/AERO.2017.7943696.
[20] Song, J., Kim, J., & Choi, W. (2011). "Design of a Low-Power Radiation Dosimeter for Satellites Using a Commercial pMOSFET." Journal of Semiconductor Technology and Science, 11(3), 197-203. doi: 10.5573/JSTS.2011.11.3.197.
[21] Pejović, S. M., Pejović, M. M., & Živanović, M. (2019). "Small dose effect in RADFET with thick gate oxide." Appl. Radiat. Isot., 152, 72–77. doi: 10.1016/j.apradiso.2019.06.034.